



## MEASUREMENT AND CONTROL OF ARCING IN A SUBMERGED-ARC FURNACE

I.J. Barker, M.S. Rennie, C.J. Hockaday and P.J. Brereton-Stiles

Mintek, Private Bag X3015, Randburg 2125, South Africa  
E-mail: [ianb@mintek.co.za](mailto:ianb@mintek.co.za)

### ABSTRACT

*This paper reports on studies that have been done on the electrical conduction in silicon, ferro silicon, and charge chrome furnaces. A system has been developed that can distinguish between normal resistive conduction and arcing, and this was used to quantify in particular the relative amount of arcing that takes place in these furnaces.*

*It was found that silicon and ferro silicon behave similarly and exhibit a relatively large amount of arcing. Charge chrome on the other hand exhibits considerably less arcing, and the extent of this arcing is highly correlated with the tapping of the furnace.*

*The arcing measurements can also be used online in the control of the furnace, both for the electrodes and electrical circuit, and for the raw materials.*

### 1. INTRODUCTION

The extent and type of arcing that takes place in a ferro-alloy furnace is directly related to the metallurgy of the process. Recently, with the advent of powerful processors in PC computers, it has become possible to study the detailed behaviour of the electrical circuit in a submerged-arc furnace in real time. For this purpose, a system known as the Arc Monitor, or "Arcmon" has been developed at Mintek, and process studies have now been done on a number of industrial furnaces using this equipment. The purpose of this paper is to briefly compare the results obtained to date on furnaces producing silicon, ferro silicon 75%, and charge chrome.

A resistor is inherently a linear circuit element, in that the instantaneous voltage across it is proportional to the instantaneous current. On the other hand, an arc is a nonlinear circuit element and consequently distorts the sinusoids of the a.c. currents flowing around the circuit of the furnace. This distortion of the waveforms thus provides information about the behaviour of the arcs in the furnace, and hence can quantify the extent of the arcing as opposed to the resistive conduction in the furnace.

The inputs to the Arcmon are the a.c. signals from the high-voltage lines on the primary side of the furnace transformers. The transformer tap positions are also monitored, in order to relate these primary-side measurements to the secondary side. There are thus no connections on the secondary side, and in particular there are no connections to the furnace hearth. The Arcmon then uses a recursive estimator to fit the circuit parameters to these waveforms. To accommodate the inherently nonlinear nature of the arc, the estimator is based in the time domain, i.e. it does not use the frequency domain and hence does not involve the use of harmonics. Also, the Arcmon runs the recursive estimator in real time, and so tracks the variations in the circuit parameters continually while the furnace is running.

### 2. THE POWER CIRCUIT OF THE FURNACE

The equivalent circuit of the furnace, as used for the Arcmon, is shown in Figure 1. In brief, it consists of a star circuit, with each individual electrode in the furnace corresponding to one of the branches of this star. Each branch then consists of a magnetic inductor, an arc, and a basic burden resistor, all in series.

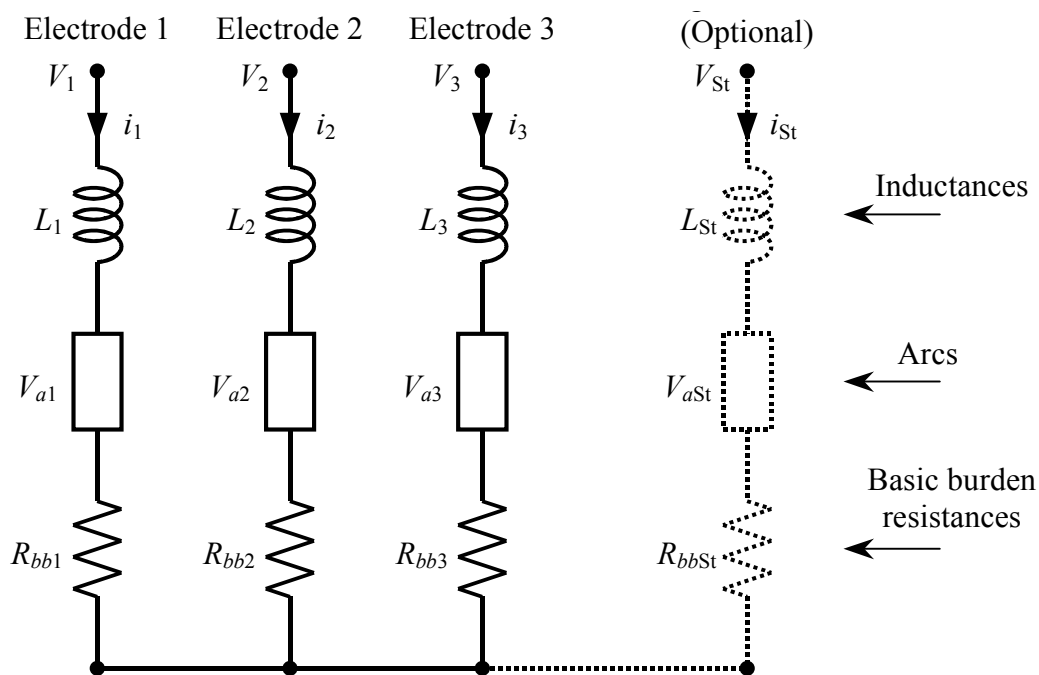


Figure 1: Equivalent circuit of furnace. This shows how the conduction through the burden can be split into an arcing component and a purely resistive component, in series. The equivalent circuit shown here excludes the delta elements that model the pulses in the transformer magnetisation currents. The Arcmon can also accommodate a stinger electrode if needed, as indicated by the dotted branch of the circuit

To distinguish between arcing and resistive conduction, an electrical model of an arc is needed. In the Arcmon, a linearised form of Cassie's model (see [3] and [4]) has been used. This would seem to provide a reasonably good fit to the observed waveforms (see below and [1]). The burden resistors are modelled by Ohm's law.

### 3. INITIAL RESULTS ON SILICON-TYPE FURNACES

The initial results obtained from using the Arcmon on silicon-type furnaces have been reported already [1]. In brief, these results can be summarised as follows:

1. The linearised form of Cassie's model was used for the arc, and the resulting waveforms generated by the circuit equations were a good match to the actual waveforms, even under extreme conditions.
2. There is a slight, but also continuously varying, asymmetry between the forward and reverse conduction under each electrode. This produces a partial rectification effect, and so gives rise to varying d.c. components in the currents. These d.c. components affect the magnetization of the steel core in each of the transformers, driving the operation of the core over the knee of the magnetization curve and into the region of magnetic saturation. The waveform of the magnetization current then develops a short sharp pulse in every cycle, around the point where the magnetization saturates. Because each transformer feeds two electrodes in the Knapsack configuration, these pulses get superimposed on the primary currents of the two phases associated with that transformer, but not on the current in the remaining third line. These delta current pulses vary sporadically and are normally fairly small, but at times may rise to exceedingly high levels. These pulses are identified, quantified, and compensated for, as part of the estimation of the circuit parameters.

3. The extent of arcing in a silicon furnace is significant. Typically, the power that is dissipated in the arcs is of the order of 20 to 60% of the total power delivered to the furnace.
4. The extent of arcing also varies continually. Although much of this fluctuation seems to be simply random, there are certain mechanisms evident. In particular, movement of an electrode hoist has a direct and immediate effect on the corresponding arc voltage. The basic burden resistance is not immediately affected by the hoist movement but may respond slightly after several minutes. The extent of arcing is also influenced by the feeding, rabbling and tapping of the furnace. One can intentionally manipulate these factors to influence the extent of arcing.

#### 4. COMPARISON OF CHROMIUM-TYPE AND SILICON-TYPE FURNACES

##### 4.1 Comparison of waveforms

Figure 2 shows an example of waveforms from a ferro-silicon furnace, while Figure 3 shows a corresponding example from a charge-chrome furnace. In each of these figures, the waveforms of the three electrode currents are shown on the upper axes, while the lower axes show the derivatives of these current with respect to time (i.e.  $di/dt$ ). These waveforms are typical of normal operation on both types of furnace.

In both these figures, the waveforms of the currents appear to be almost pure mains-frequency sinusoids, but the derivatives enhance and hence reveal significant distortions around the basic sinusoids. The arcs in the circuit are the source of these distortions. In the process of differentiating a sinusoidal waveform, a phase shift of  $\pi/2$  radians ( $=90^\circ$ ) is produced (i.e.  $d/dx(\sin[x]) = \cos[x] = \sin[x + \pi/2]$ ), and so the peaks of each  $di/dt$  waveform synchronise with the zero crossings of the corresponding current waveform. Thus the slight dent in each peak of the  $di/dt$  is associated with the arc in that phase being re-started after the zero-crossing of its

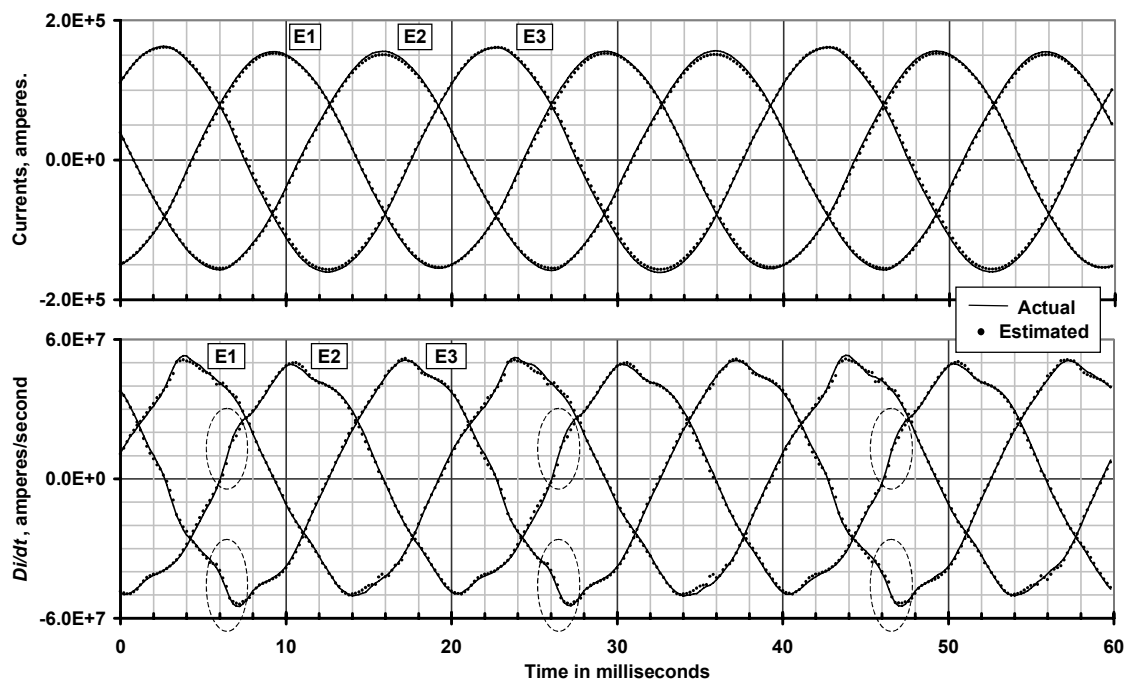


Figure 2: Waveforms from a 75% ferro-silicon furnace. This figure shows the waveforms of the electrode currents on the upper set of axes, and the derivatives (i.e.  $di/dt$ ) of these currents on the lower set of axes. These waveforms are from a ferro-silicon furnace dissipating around 25 to 30 MW. The presence of arcing in the furnace reveals itself by the distortion of particularly the  $di/dt$  waveforms. In this example, a small amount of delta current pulsing (see text) is also occurring between electrodes 2 and 3, as encircled

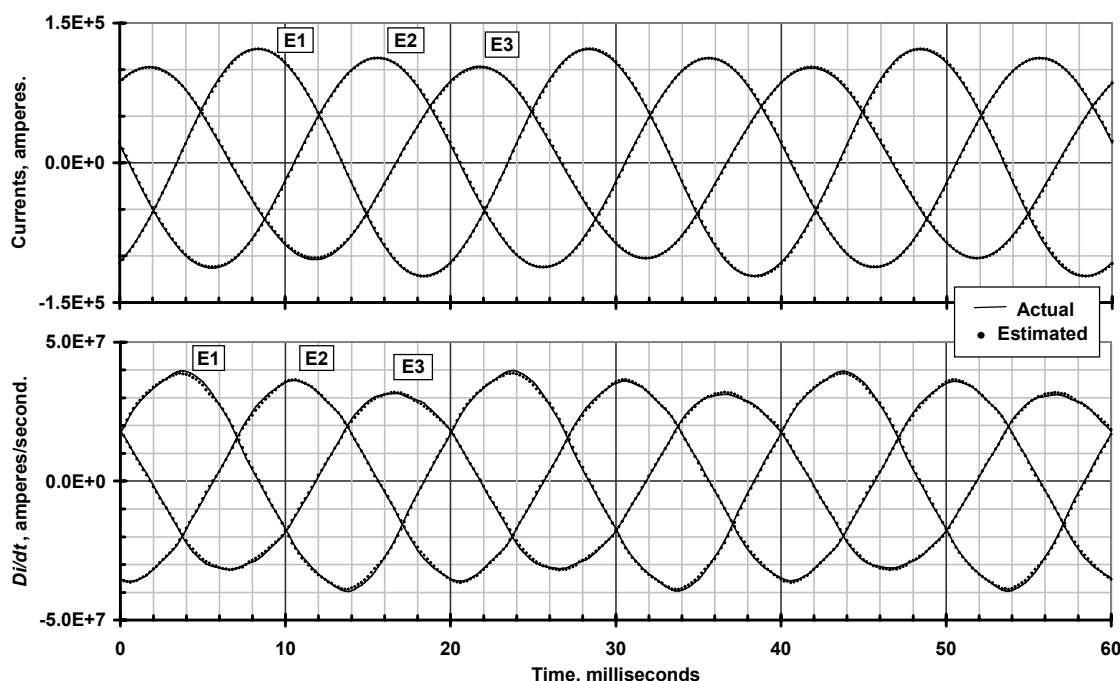


Figure 3: Waveforms from a charge-chrome furnace. These waveforms are from a charge chrome furnace dissipating about 45 to 50 MW. In comparison with Figure 2, it is very evident that the distortion of the  $di/dt$  waveforms here is significantly less than in the ferro-silicon furnace

current. Hence the magnitude of the dent in the peak of the  $di/dt$  is a visual indication of the extent of arcing in that phase.

When comparing Figures 2 and 3 in this way, it is very evident that there is considerably more arcing in the ferro-silicon furnace than in the charge-chrome furnace.

Furthermore, in Figure 2, a small amount of delta current pulsing (see paragraph 2 under “Initial results on silicon-type furnaces” above) is evident. In this particular example, it can be seen on the  $di/dt$  waveforms of electrodes 2 and 3 as small steep jumps, as encircled in the Figure. The presence of this delta current pulsing indicates that asymmetrical conduction in the arcs also takes place in ferro-silicon furnaces, much as it was found to do in silicon furnaces. The Arcmon has detected this delta current pulsing in charge-chrome furnaces as well, but with somewhat smaller magnitudes that are not as easily seen on the waveforms.

#### 4.2 Comparison of the arc-voltage magnitudes (parameter $V_a$ )

The waveform of the voltage across an arc in a furnace is normally a slightly skewed square wave with rounded edges. When Cassie’s model is used to describe the arc, the parameter  $V_a$  is approximately the magnitude of this square wave. (In some extreme cases, particularly where the operation is very unbalanced, the arc waveform may become distorted but  $V_a$  continues to provide a measure of the magnitude of the arc.)

Figures 4 and 5 show typical examples of the evolution of  $V_a$  over a period of 24 hours, with Figure 4 for ferro silicon and Figure 5 for charge chrome. For clarity, only one of the phases from the corresponding furnace is shown in each of these two Figures. Also, the Arcmon estimator has a lower limit that prevents the estimate of  $V_a$  going to zero, which is why the traces on the graphs never actually touch the horizontal axis. Again, it is clearly evident that there is far less arcing in the charge-chrome furnace than in the ferro-silicon furnace.

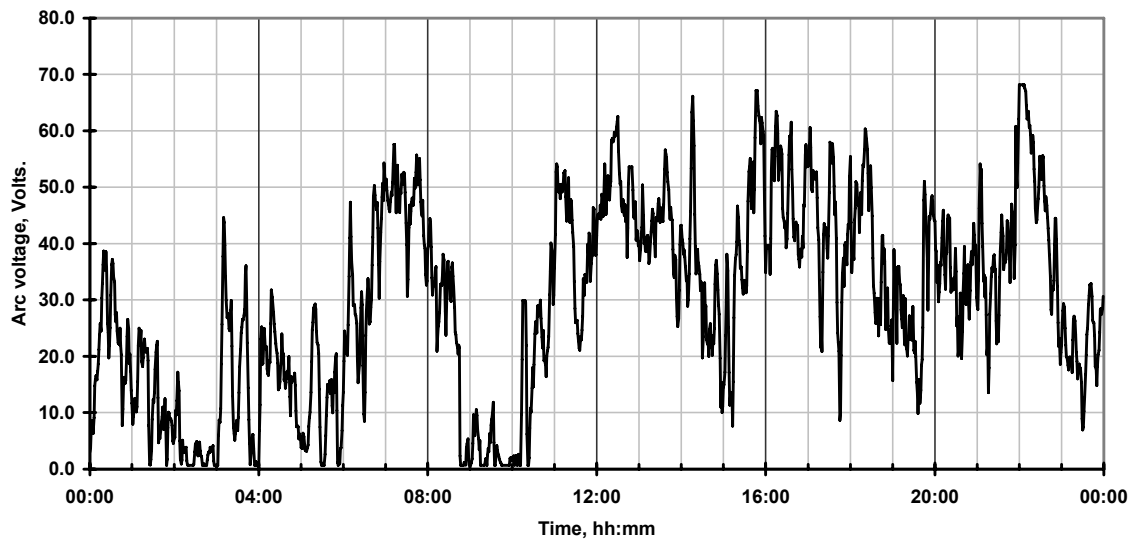


Figure 4: Magnitude of the arc voltage in a ferro-silicon furnace: typical graph over 24 hours. This graph shows the estimate of the parameter  $V_a$  from Cassie's model, for one electrode in a ferrosilicon furnace, over a period of 24 hours. (Visually, the waveform of the voltage across an arc looks like a slightly skewed square wave with rounded edges. In Cassie's model for an arc, the parameter  $V_a$  is approximately the magnitude of this square wave.)

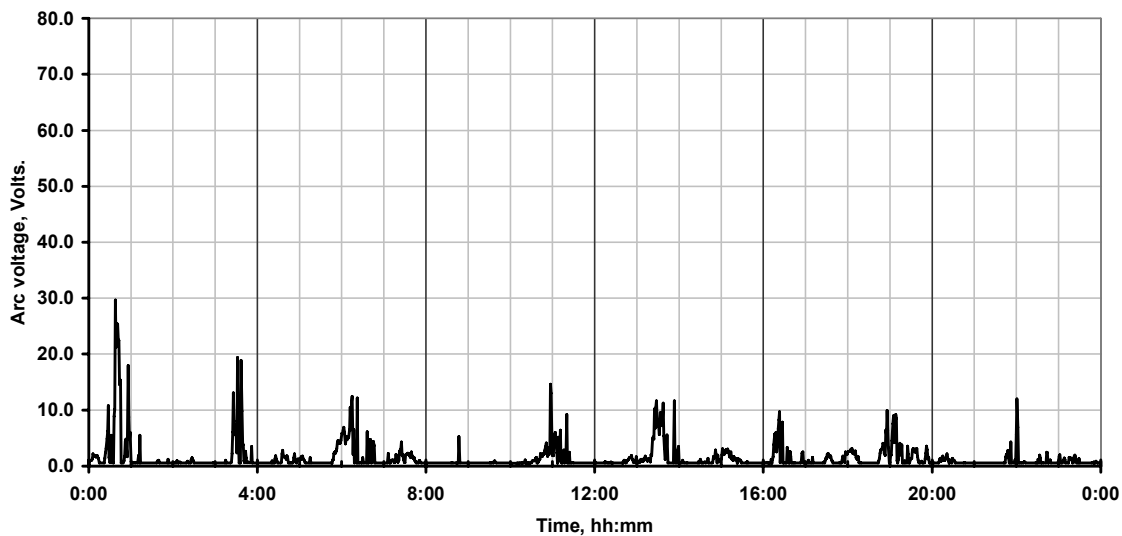


Figure 5: Magnitude of the arc voltage in a charge-chrome furnace: typical graph over 24 hours. This shows the estimated parameter  $V_a$  on the same vertical scale as in Figure 4. This figure also highlights the fact that there is normally a lot less arcing in a charge-chrome furnace

In the case of ferro silicon (i.e. Figure 4), there are a few short periods where  $V_a$  drops to virtually zero, but most of the time  $V_a$  lies within a band of about 20 to 50 volts. There is also a significant amount of random noise on this signal. This is fairly similar to a silicon furnace, as shown in [1].

In the case of charge chrome (i.e. Figure 5), the arcing tends to occur in bursts. These bursts are associated with the tapping of the metal and slag from the furnace. In between these bursts, the arc voltage is virtually

zero. The extent of arcing during these bursts can vary, normally rising to peaks of about 10 to 20 volts, but occasionally rising much higher.

### 4.3 Comparison of the arc power fractions

The Arcmon unit is also able to calculate the amount of power dissipated in each of the arcs and each of the resistors of the equivalent circuit of a furnace. Through this it is able to calculate the fraction of the total power to the furnace that is dissipated in the arcs, which we will here term the “arc power fraction”. This is another measure that can be used to compare the amount of arcing between the different processes. The usefulness of this arc power fraction as a measurement, as opposed to the individual  $V_a$  or  $Rbb$  signals, arises from the fact that it is a single quantity for the furnace as a whole, and it is independent of the power or current levels in the furnace. It also has a direct metallurgical relevance as to how the energy dissipation is split between the various zones within the burden of the furnace.

In this way, Figure 6 shows a typical arc power fraction for a ferro-silicon furnace over 24 hours, and Figure 7 shows the same for a charge-chrome furnace.

Perhaps not surprisingly, the magnitude of the arc power fraction in the ferro-silicon furnace is similar to that in the silicon furnace shown in [1], i.e. it is of the order of 20% to 60%.

In the case of charge chrome, the arc fraction is much lower and comes in bursts that follow the tapping of the furnace, similar to the trend of the  $V_a$  for charge-chrome furnaces as shown in Figure 5.

## 5. DISCUSSION

It is very evident from Figures 2 to 7 that normally there is significantly less arcing in a charge-chrome furnace than in a ferrosilicon furnace. Furthermore, in a charge-chrome furnace, there is a burst of increased arcing for about 1 hour after each tap, whereas in a ferro-silicon furnace this behaviour is not readily observed.

### 5.1 Ferro-silicon and silicon furnaces

The amount of arcing in a ferro-silicon furnace (see Figure 6) is similar to the amount (about 20% to 60%) reported in [1] for a silicon furnace. The apparently random way in which the arc power fraction varies is also similar. Furthermore, although the results are not presented here, the response to an electrode being moved is similar as well.

Metallurgically, the ferro-silicon process is similar to the silicon process in that there is a crater around the tip of each electrode, in which the arc is located. There is not normally any significant slag layer. The silicon process is comprehensively discussed in [8]. It is not surprising then that both types of furnace behave similarly from the perspective of arcing and related electrical behaviour.

While the arcing takes place in the crater zone, the resistive power dissipation presumably takes place elsewhere within the burden of the furnace. The extent to which the power is split between these two zones has implications for the metallurgy of the process, and hence the efficiency of the furnace. This is currently under investigation.

### 5.2 Charge-chrome furnaces

Charge-chrome furnaces in the industry can vary from a typically low resistance operation to a relatively high resistance operation. The purpose of having a high resistance operation is to facilitate an increase in power delivery within the same electrical constraints for a given furnace installation. Levels of arcing that were observed many years ago on furnaces with lower resistances [7], were significantly more than the levels observed in the present study, which has been done to date on furnaces with higher resistances.

The charge-chrome process [5] has a significant quantity of slag in the furnace. Floating on top of this slag layer there is reportedly a “carbon bed”, also called a “coke bed”. Some mixing between the slag and this carbon bed presumably occurs during normal operation, although this is not evident from post-mortem stud-

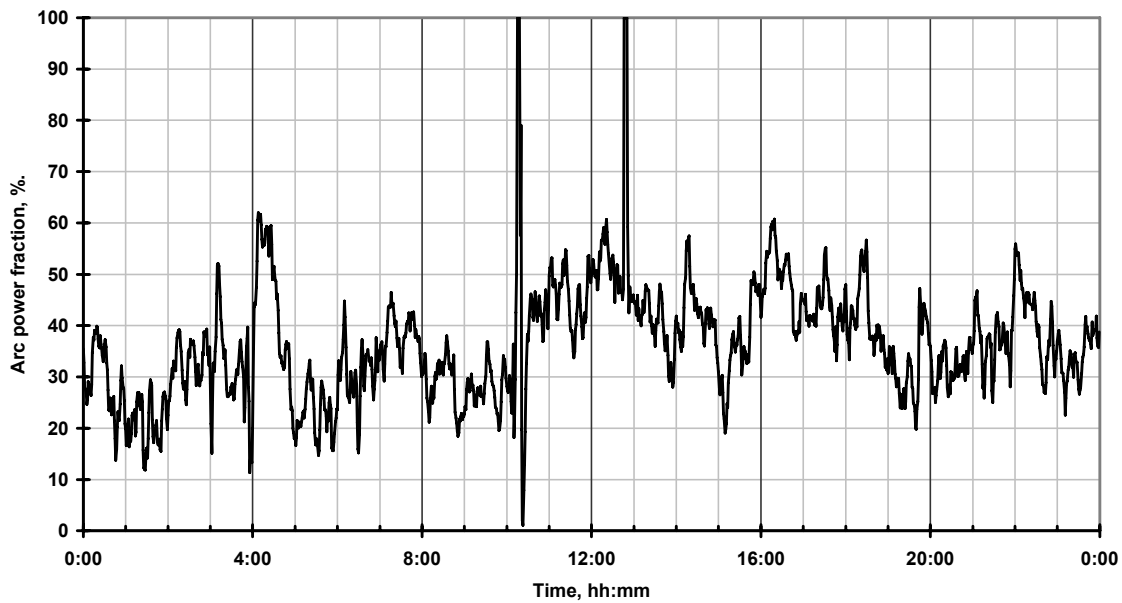


Figure 6: Typical arc power fraction in a ferro-silicon furnace, over 24 hours. The arc power fraction is the fraction of the total power to the furnace that ends up being dissipated in the arcs

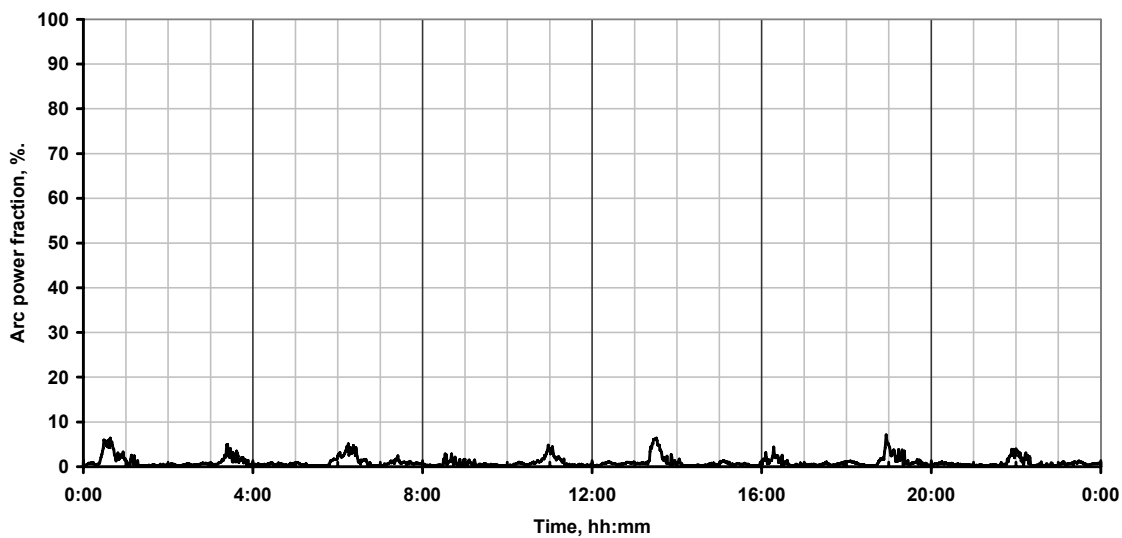


Figure 7: Typical arc power fraction in a charge-chrome furnace, over 24 hours. This graph is purposefully drawn with the same vertical scale as that in Figure 6, to emphasize the significant difference in the relative amount of arcing between the two types of furnace. Note how the arcing comes in bursts, which are synchronised with the tapping of alloy and the slag from the furnace

ies. Arcing is not likely to occur much in conjunction with a slag layer, but it can be expected to occur more easily within a coke bed, and between a coke bed and the tip of an electrode. Therefore, the low amount of arcing measured by the Arcmon in the period preceding a tap is probably associated with the bulk of the carbon bed being located higher up in the furnace than the tips of the electrodes, so that the conduction takes place through a zone that contains predominantly slag.

During the tap, as slag and metal are removed, cooler particulate material from the carbon bed and the raw materials descend in the furnace. The observed increase in the amount of arcing after tapping the furnace is probably associated with a significant portion of this particulate material entering the conduction zone beneath the electrodes. After the tap hole is closed, the smelting taking place in the furnace slowly increases the depth of this slag layer until, after an hour or so, the carbon layer again rises above the level of the tips of the electrodes and the amount of arcing decreases.

Electrode tip breaks also lead to significantly higher levels of arcing for extended periods (often up to 1 to 2 days), until the electrode can be slipped sufficiently for the tip to return to its original position in the furnace.

In this type of smelting process, higher temperatures in the reduction zone will enhance the reduction of the more refractory oxides, in particular that of silicon. This will increase the percentage of these elements in the final alloy that gets tapped. In particular, the % Si in the metal will increase. The extent of arcing does affect the temperature distribution in the reaction zone, and this is currently under investigation.

### 5.3 Arc voltages and arc lengths

Bowman [2] reviews correlations between arc length and voltage in d.c. furnaces. In this case, arc voltages around 20 to 50 volts correspond to arc lengths from a couple of millimetres up to about 100 millimetres. Although it is questionable as to what extent such correlations can be applied to a.c. furnaces, it seems reasonable to assume that they will not be too dissimilar. This would mean that the arc gaps in the craters beneath the tips of the electrodes in a ferro-silicon furnace would be typically up to about 100 mm long. This agrees with the changes that we have seen in the estimated  $V_a$  when the corresponding electrode is moved. It also suggests that, from the very low  $V_a$  voltages that are observed in charge-chrome furnaces, the arcing taking place in such furnaces is over very short lengths – probably little more than just adjacent conductive particles brushing past each other.

## 6. USE OF ARCING INFORMATION IN THE CONTROL OF THE FURNACE

Clearly the mode of electrical conduction in silicon and ferro-silicon furnaces is very different from that in charge-chrome furnaces, particularly in terms of arcing. Consequently the approach to control of these two types of process is somewhat different.

### 6.1 Silicon and ferro silicon

In the case of silicon and ferro-silicon, the movement of an electrode quickly and directly affects the Arcmon estimate of the corresponding  $V_a$  parameter. Hence  $V_a$  can be controlled through the movement of the corresponding electrode. While it is possible to control an electrode's movement directly from  $V_a$ , we have found it more practical to use a cascade arrangement, in which the parameter from the Arcmon is used to modify the resistance set point of the Minstral [6] resistance controller, and the Minstral's resistance control algorithm then adjusts the electrode position.

Allowing the resistance set points to vary in this way can affect the power delivered to the furnace, causing variations both upwards as well as downwards. Such variations may temporarily affect the rate of production of alloy in the furnace, although they do tend to average out over longer periods. Consequently it is necessary to constrain the allowable variation in the resistance set points that are sent to the Minstral. The extent of freedom within the constraints of the electrical operating region of the furnace plays an important part in this, and varies from one furnace to another. One of the reasons for cascading the control onto the Minstral is that the Minstral then automatically maintains the overall operation within safe electrical limits.

The control of the electrodes, the raw materials, the tapping of the alloy from the furnace, as well as a number of other inputs into the operation of the furnace, are all an integral part of the overall furnace operation. In a silicon or ferro-silicon furnace in particular, no one aspect can be viewed in isolation. Consequently, Mintek is currently investigating other approaches to the control that facilitate a more global perspective.



The Arcmon contributes to this by providing unique information about the electrical side of the metallurgy, which was not previously available.

## 6.2 Charge chrome

Because the amount of arcing in the charge-chrome furnaces studied to date is very low for extended periods, there is no basis for any automatic control of the electrodes based on measurements of  $V_a$ , as described above for silicon and ferro-silicon furnaces. This is especially the case where the electrode hoists are allowed only limited movement. However, for other ferro-chrome furnaces that have higher arc fractions, it may be possible to do such control.

The sudden loss of an electrode tip in a large ferro-chrome furnace with restricted electrode movement results in a sudden sustained increase in the level of arcing beneath the affected electrode. Information from the Arcmon identifies this unequivocally.

Arcmon parameters correlate with some of the furnace operating variables, and can be used for predictions. The raw materials, particularly the carbon balance, affect the Arcmon variables. These areas are also still under investigation currently.

## 7. CONCLUSIONS

1. In terms of electrical conduction, silicon and ferro-silicon furnaces behave very similarly, but are very different from charge-chrome furnaces.
2. The modern charge-chrome furnaces that were studied exhibited relatively low levels of arcing, but the extent of arcing increased for a short time after each tapping of the furnace. Electrode tip losses also increased the amount of arcing. This evidence suggests that the carbon bed is normally located relatively high up in the furnace, so that most of the conduction takes place through slag, as there is only a relatively small quantity of carbonaceous reductant in the main conduction paths beneath the electrodes.
3. In silicon and ferro-silicon furnaces, the measurement of the arc voltage parameter  $V_a$  can be used to control the electrode hoists. In the charge-chrome furnaces studied, because  $V_a$  is often virtually zero for long periods of time, the use of this parameter for the automatic control of the electrodes is impractical, but the information may still be usable for controlling other process variables, and for the detection of tip losses. The benefits of all these forms of control are presently still being studied and quantified.

## 8. ACKNOWLEDGEMENTS

The authors would like to thank the companies and the staff of the various plants with which they have worked during the course of this study.

This paper is published by permission of Mintek.

## REFERENCES

- [1] Barker, I. J., Rennie, M. S., Hockaday, C. J., Brereton-Stiles, P. J., *Modes of electrical conduction in industrial silicon-type furnaces*, Silicon for the Chemical Industry VIII, Trondheim, Norway, 12-16 June 2006. Eds: H. A. Oye, H. Brekken, T. Foosnes, L. Nygaard. NTNU Tapir Forlag, 2006. Pp79-90.
- [2] Bowman, B., *Properties of arcs in dc furnaces*, 52<sup>nd</sup> Elec. Furn. Conf. (Nashville Meeting, Nov. 13-16, 1994). Iron and Steel Society, Inc, 1995, p 111-120.
- [3] Brown, T. E., *The electric arc as a circuit element*, J. Electrochem. Soc., **102**, 1955, p 27-37.
- [4] Cassie, A. M., *Arc rupture and circuit severity a new theory*, Internat. Conf. on Large Electric High Tension Systems, Paris, 1939, p 1-14.
- [5] Habashi, F., *Handbook of Extractive Metallurgy*, Vol 1, Wiley\_VCH, 1997
- [6] Minstral: see Mintek's StarCS webpage on [www.starcs.co.za](http://www.starcs.co.za)

- [7] Rennie, M. S., *The application of on-line data and the development of models relating to the production of charge chrome*. Proc. Elec. Furn. Conf., Vol. 37 (Detroit Meeting, 1979), Iron and Steel Society of AIME, 1979, pp 202-209.
- [8] Schei, A., Tuset, J. Kr., Tveit, H., *Production of high silicon alloys*, Tapir Forlag, Trondheim, 1998.